Soils and Foundations 2013;53(6):879–893

The Japanese Geotechnical Society

Soils and Foundations

www.sciencedirect.com
journal homepage: www.elsevier.com/locate/sandf

Normalized shear modulus reduction and damping ratio curves of quartz sand and rhyolitic crushed rock

Kostas Senetakis[a,*], Anastasios Anastasiadis[b], Kyriazis Pitilakis[b]

[a]*School of Civil Engineering and Technology, Sirindhorn International Institute of Technology (SIIT) Thammasat University, Rangist Campus, Pathum Thani 12120, Thailand*
[b]*Department of Civil Engineering, Aristotle University of Thessaloniki, Greece*

Received 27 June 2012; received in revised form 31 July 2013; accepted 28 August 2013
Available online 22 November 2013

Abstract

This paper presents a laboratory investigation of the strain-dependent dynamic properties of volcanic granular soils composed of a rhyolitic crushed rock along with additional experiments on quartz sand through a high-amplitude resonant column testing program. The sands were tested in a dry state in torsional mode of vibration and thus the degradation of the normalized shear modulus and the increase of damping ratio in shear as a function of the shear strain amplitude (γ) were examined. It was revealed that, for a given mean effective confining pressure (σ'_m) and coefficient of uniformity (C_u), the volcanic sands showed higher linearity in comparison to the quartz sands and that this trend became more pronounced with decreasing σ'_m and increasing C_u. In contrast to the general trend observed in the quartz soils, the confining pressure and the grain-size characteristics hardly affected the rate of normalized modulus degradation and damping increase in the volcanic sands. These differences are possibly related to the micro-mechanisms that dominate at particle contacts in the range of small to medium shear strain amplitudes. For example, the possible more pronounced crushing of the asperities during the elevation of the confining pressure and during the dynamic loading along with the lower inter-particle friction angle and stiffness of the volcanic sands of crushable particles in comparison to the quartz sands of stronger particles might play an important role in the energy dissipation during the dynamic excitation and thus on the rate of damping increase or modulus degradation.

1. Introduction

The small-strain shear modulus (G_O) along with the normalized modulus degradation (G/G_O) and damping ratio increase (D) from small to large shear strains (γ) are key parameters for seismic response analysis studies. In geotechnical engineering practice, the strain-dependent dynamic properties of soils, commonly expressed in terms of the G/G_O-log γ and D-log γ curves used directly in one- or two-dimensional computer codes for seismic response analysis studies, as for example the SHAKE (Schnabel et al., 1972) and the QUAD4M (Idriss et al., 1973, Hudson et al., 1994), are derived from available-literature data on similar materials. For example, it is common practice to adopt in computer programs the proposed upper and lower bounds of the G/G_O-log γ and D-log γ curves by Seed and Idriss (1970), Seed et al. (1986) or Rollins et al. (1998) with respect to granular soils, or the corresponding curves by Sun et al. (1988), Vucetic and Dobry (1991) or Stokoe et al. (2004) with respect to soils of variable plasticity index. Alternatively, analytical models or equations of empirical form are often utilized in computer programs, where the normalized

*Corresponding author. Tel.: +66 2 986 9009, +66 2 986 9101, +66 2 564 3226x1912, Mobile: +66 89 191 7624.
E-mail address: ksenetak@siit.tu.ac.th (K. Senetakis).
Peer review under responsibility of The Japanese Geotechnical Society.

Production and hosting by Elsevier

0038-0806
http://dx.doi.org/10.1016/j.sandf.2013.10.007

shear modulus and the damping ratio are commonly expressed as a function of the shear strain amplitude, γ, the mean effective confining pressure, σ'_m, as well as soil parameters such as the plasticity index, PI, and the coefficient of uniformity, C_u.

Two of the most commonly used analytical models in soil dynamics concern the hyperbolic model originally proposed by Hardin and Drnevich (1972a, 1972b) and later in a modification form by Darendeli (1997, 2001) as well as the Ramberg–Osgood model (Anderson, 1974). For both granular and cohesive soils and for a given shear strain amplitude, the damping ratio, D, is usually determined from the corresponding G/G_O through simple one- or two-order polynomial relationships or exponential expressions (e.g., Khouri, 1984, Zhang et al., 2005, Aggur and Zhang, 2006, Okur and Ansal, 2007). A more sophisticated model, where the soil is assumed to exhibit Masing behavior, has been also presented in a modification form by Darendeli (2001). In his study, Darendeli determined a series of fitting parameters from experimental data on intact soils of variable plasticity index. This model was later verified for granular soils by Menq (2003).

Overall, the most important parameter that affects the G/G_O-log γ and D-log γ curves of granular soils and can be used for a useful quantification and prediction of the dynamic response of the ground and the corresponding earthquake-induced deformations is the mean effective confining pressure, σ'_m. The increase of σ'_m leads to more linear shape of the curves, that is higher G/G_O and lower D values at a given shear strain (e.g., Shibata and Soelarno, 1975; Sherif and Ishibashi, 1976; Iwasaki et al., 1978; Tatsuoka and Iwasaki, 1978; Kokusho, 1980, 2004; Khouri, 1984; Tanaka et al., 1987; Saxena and Reddy, 1989; Menq, 2003, Xenaki and Athanasopoulos, 2008; Anastasiadis et al., 2011). Along with the mean effective confining pressure, in recent studies it was revealed that the coefficient of uniformity (C_u) plays an important role on the cyclic response of granular soils. It has been shown that the increase of C_u leads to higher non-linearity in the range of medium to high strain levels (e.g., Menq, 2003; Anastasiadis et al., 2011; Wichtmann et al., 2011; Senetakis, 2011), a trend not quantitatively supported in previous studies on granular materials (e.g., Seed and Idriss, 1970; Seed et al., 1986; Rollins et al., 1998). In addition, Anastasiadis et al. (2011) and Senetakis (2011) reported that for a given soil type, the uniform to poor graded sands have slightly more linear G/G_O-log γ and D-log γ curves in comparison to the uniform gravelly soils and that for sands with mean grain size (d_{50}) below 2.00 mm, parameter d_{50} also affects the rate of modulus degradation and increase in damping, a trend not observed by Menq (2003) and Wichtmann et al. (2011).

The research relative to the dynamic and pre-failure response of geo-materials mentioned above has been focused on soils predominantly composed of quartz particles. However, it is questionable whether the available experimental data and proposed G/G_O-log γ and D-log γ curves derived from laboratory investigations on quartz soils, are appropriate for use in the seismic design of structures and geo-structures where volcanic soils are used. Recent failures of slopes and geo-structures (e.g., Orense et al., 2006; Kazama et al., 2012; Kawamura and Miura, 2013) have underlined the importance for further laboratory investigations and a better understanding of the engineering behavior of volcanic soils which have been characterized in the literature as "non-textbook" geo-materials (e.g., Rouse et al., 1986; Wesley, 2003; Orense et al., 2006), while the research works relative to the mechanics and dynamics of volcanic soils with intra-particle voids are relatively limited (e.g., Meyer et al., 2005; Orense et al., 2006; Pender et al., 2006). In this direction, Anastasiadis et al. (2010), Senetakis (2011) and Senetakis et al. (2012a), (2013a) have shown that the available relationships that predict the pre-failure response of soils predominately composed of quartz particles are not valid for volcanic granular materials in both the range of very small and small to medium strain levels. In the experimental study by Senetakis et al. (2013a) it was also revealed that at small to medium strain amplitudes the response of a pumice soil of crushable particles was more linear in comparison to the response of quartz soils of strong particles and similar grading. They partially attributed this behavior to the possibility of more pronounced micro-crushing of the asperities in the pumice soil, since micro-crushing affects the dissipation of energy and the overall different particle contact responses between pumice and quartz soils.

This paper contributes to partially fill the literature gap relative to the dynamic properties of volcanic granular soils by analyzing the high-amplitude resonant column test (HARCT) results of volcanic sands composed of a rhyolitic crushed rock. The HARCT results are enhanced with additional experimental data derived from quartz sands. All the experiments were carried out in the Laboratory of Soil Mechanics, Foundations and Geotechnical Earthquake Engineering of Aristotle University in Thessaloniki, Greece.

2. Materials and methodology

2.1. Materials used

In this experimental investigation, 13 fine to coarse grained sands of variable types were studied. All materials were prepared in the laboratory following typical procedures; washing of the parent soil on sieve No200 (75 μm), oven dry and construction of specific grain-size distribution sands through a series of sieves. The grading curves of the 13 sands are shown in Fig. 1 which figure was also presented by Senetakis et al. (2012a). The compaction characteristics and shear strength parameters of the materials under study have been thoroughly presented by Senetakis (2011) and briefly discussed by Senetakis et al. (2012a).

Four materials, namely N1, N2, N3 and N4 comprise fractions of a medium grained, poor graded natural sand of sub-rounded to rounded particles. These sands have a mean grain size (d_{50}) and a coefficient of uniformity (C_u) in a range of 0.27–1.33 mm and 1.34–2.76, respectively. Four sands, namely Q1, Q2, Q3 and Q4, comprise fractions of well graded sandy gravel of sub-angular to angular particles having values of d_{50} and C_u in a range of 0.16–2.00 mm and 2.00–3.23, respectively. These soils are predominately composed of quartz particles with specific gravity of solids, G_s, equal to

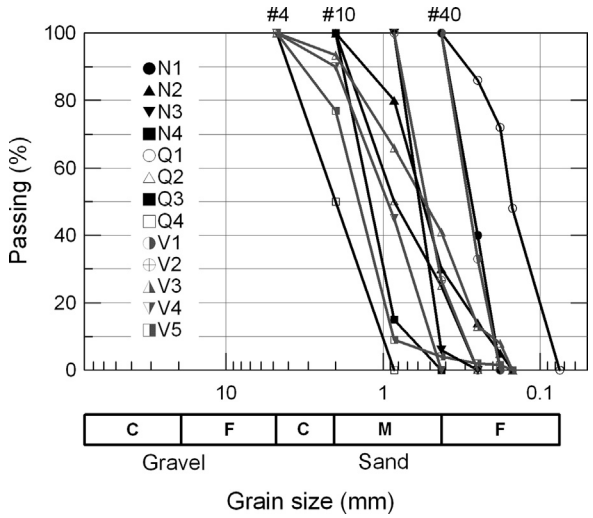

Fig. 1. Grain-size distribution curves of materials used. (Note: Materials N4 and Q3 have the same grain-size distribution curve.)

2.67 (Senetakis, 2011; Senetakis et al., 2012a). Finally, five materials, namely V1, V2, V3, V4 and V5, included in this study, comprise fractions of a rhyolitic-glassy rock (volcanic artificially crushed rock). These sands have sub-angular to angular crushable particles of intra-particle voids with specific gravity equal to 2.36 (Senetakis, 2011; Senetakis et al., 2012a). The grain-size distribution parameters of d_{50} and C_u range between 0.23–1.60 mm and 1.53–4.18, respectively.

2.2. Experimental equipment and sample preparation

The dynamic testing program of low to high shear strain amplitude measurements was performed in a Long-Tor resonant column (RC) apparatus that follows the fixed-free configuration (Drnevich, 1967) on dry specimens of approximately 71 mm in diameter and 142 mm in height. Comprehensive description of the experimental equipment has been given by Senetakis (2011), Anastasiadis et al. (2012) and Senetakis et al. (2012a, 2012b, 2012c, 2013a).

The specimens were prepared into a metal mold of appropriate dimensions in the RC device using variable compaction energy. Dense and medium dense specimens were constructed in many layers of equal dry mass and each layer was compacted gently in order to avoid particle breakage, using a metal rod of diameter half the diameter of the specimen. Loose specimens were constructed by hand-spooning of the dry material into the metal mold.

2.3. High amplitude resonant column testing (HARCT) program

In twenty-one (21) specimens of variable mineralogy (quartz and volcanic), particle shape, grain-size distribution and void ratio, constructed in the laboratory, high-amplitude resonant column tests (HARCT) were performed at least at two levels of the mean effective confining pressure, σ'_m. Table 1 summarizes the aforementioned 21 dry specimens, the initial values of dry unit weight (γ_{do}) and void ratio (e_o) at which specimens were prepared and the mean effective confining pressures (σ'_m) at which HARCT were performed. In particular, low-amplitude RC measurements along with HARCT measurements were performed at increasing steps of σ'_m following the sequence 25, 50, 100 and finally 200 kPa of σ'_m. At each step of confining pressure, samples were allowed to equilibrate for about 40–60 min, in most cases before the performance of the RC tests. During that period of time, small-strain stiffness measurements were undertaken at intervals of about 5–10 min. In general a slight increase of small-strain stiffness was observed at first. A stabilization of the stiffness was an indication of sample equilibrium and at that moment, low-amplitude and HARCT measurements were carried out. After the performance of HARCT at a given confining pressure, there was allowed a period of time of about 15–60 min for the samples to recover at least 95% of their initial stiffness, before the increase of the pressure for RC records at a higher level of σ'_m. After the performance of HARCT measurements at the highest confining pressure of 200 kPa, in most samples, the pressure was gradually decreased and checks of the small-strain stiffness and damping were undertaken. It is noticed that despite the large number of imposed loading cycles to the samples and that the HARCT were performed at elevated confining stresses, in both the quartz and the volcanic sands no significant change of the small-strain stiffness and damping during the reversal of the confining pressure was observed. This is because, despite

Table 1
High amplitude torsional resonant column testing (HARCT) program.

Code name of specimen	Laboratory material	d_{50} (mm)	C_u	γ_{do} (kN/m^3)	e_o	σ'_m for HARCT (kPa)
(1)	(2)	(3)	(4)	(5)	(6)	(7)
N1-1	N1	0.27	1.58	15.8	0.661	50, 100, 200
N1-2	N1	0.27	1.58	13.3	0.964	100, 200
N2-3	N2	0.56	2.76	16.5	0.588	25, 50, 100, 200
N2-4	N2	0.56	2.76	15.6	0.682	25, 50, 100
N3-1	N3	0.60	1.34	15.6	0.680	100, 200
N3-2	N3	0.60	1.34	13.5	0.938	100, 200
N4-2	N4	1.33	2.13	16.7	0.571	100, 200
N4-3	N4	1.33	2.13	16.5	0.588	50, 100, 200
Q1-1	Q1	0.16	2.00	15.6	0.683	50, 100, 200
Q1-2	Q1	0.16	2.00	13.4	0.954	50, 100
Q2-1	Q2	0.85	3.23	17.0	0.545	25, 100, 200
Q3-1	Q3	1.33	2.13	16.4	0.594	25, 100, 200
Q3-2	Q3	1.33	2.13	14.4	0.820	100, 200
Q4-1	Q4	2.00	2.50	16.9	0.553	25, 50, 100
Q4-2	Q4	2.00	2.50	14.8	0.770	25, 50, 100
V1-1	V1	0.23	1.53	12.7	0.823	50, 100, 200
V2-1	V2	0.53	2.23	11.8	0.961	25, 100
V2-2	V2	0.53	2.23	10.3	1.250	25, 100
V3-2	V3	0.55	4.18	12.2	0.898	100, 200
V4-1	V4	0.92	2.00	11.9	0.943	50, 100
V5-1	V5	1.60	2.12	11.7	0.976	50, 100

(2) N_i=natural quartz sand, Q_i=quarry quartz sand, V_i=volcanic sand.
(3) Mean grain size (4) Coefficient of uniformity $C_u=d_{60}/d_{10}$.
(5) Initial dry unit weight at which specimens were prepared.
(6) Initial void ratio at which specimens were prepared.
(7) Mean effective confining pressures at which high amplitude RC tests were performed.

the plastic deformations occurred in the soil mass during the elevation of σ'_m or during the torsional excitation, the RC testing is a non-destructive method capable of studying the stiffness and damping of geo-materials from very small to medium strain amplitudes and at elevated confining stresses.

In total, 53 complete series of HARCT were performed on 21 specimens in a range of mean effective confining pressures from 25 to 200 kPa and a range of shear strain amplitudes from 2.7×10^{-4}% to 5.4×10^{-2}%. The resonant column tests and the analysis of the experimental results were performed according to the specifications of ASTM (1992) (ASTM D4015-92). It should be noted that it was decided that an upper bound of confinement (σ'_m) equal to 200 kPa was adopted in the experiments because in general the volcanic sands have crushable-weak particles and in this study we focused on the dynamic properties of dry sands for which no significant changes of the grading curve is observed during the elevation of σ'_m. In addition, a significant change of the grading of the sands because of breakage could affect the accurate determination of the void ratio in the volcanic sands with intra-particle voids. This paper focuses on the non-linear response of the quartz and the volcanic sands, whilst the low-amplitude RC test results along with interpretations and proposed equations for the small-strain shear modulus and damping ratio are thoroughly presented by Senetakis et al. (2012a).

3. Experimental results and proposed relationships

3.1. Synopsis of experimental HARCT results and analytical models used

Representative HARCT results are given in Figs. 2 and 3. Fig. 2 refers to quartz sands whilst Fig. 3 refers to volcanic sands. In the same figures, the theoretical G/G_O-log γ and D-log γ curves proposed by Menq (2003) for granular soils are also plotted for comparison purposes.

Based on the well-known modified hyperbolic model for the estimation of the G/G_O-log γ curves, and the modified "Masing behavior" model for the estimation of the D-log γ curves (originally proposed by Darendeli, 2001), Menq (2003) proposed analytical relationships for the estimation of the non-linear dynamic properties of sandy and gravelly soils. The modified hyperbolic model is given analytically in Eq. (1), where the fitting parameters of reference strain (γ_{ref}), which corresponds to the shear strain for $G/G_O=0.5$, and coefficient of curvature (a), as proposed by Menq (2003), are given in Eqs. (2) and (3), respectively, as a function of the mean effective confining pressure (σ'_m) and the coefficient of uniformity (C_u), and P_a in the same equations refers to the atmospheric pressure. In particular, Menq found that the constant parameter A_γ of Eq. (2) may be estimated through

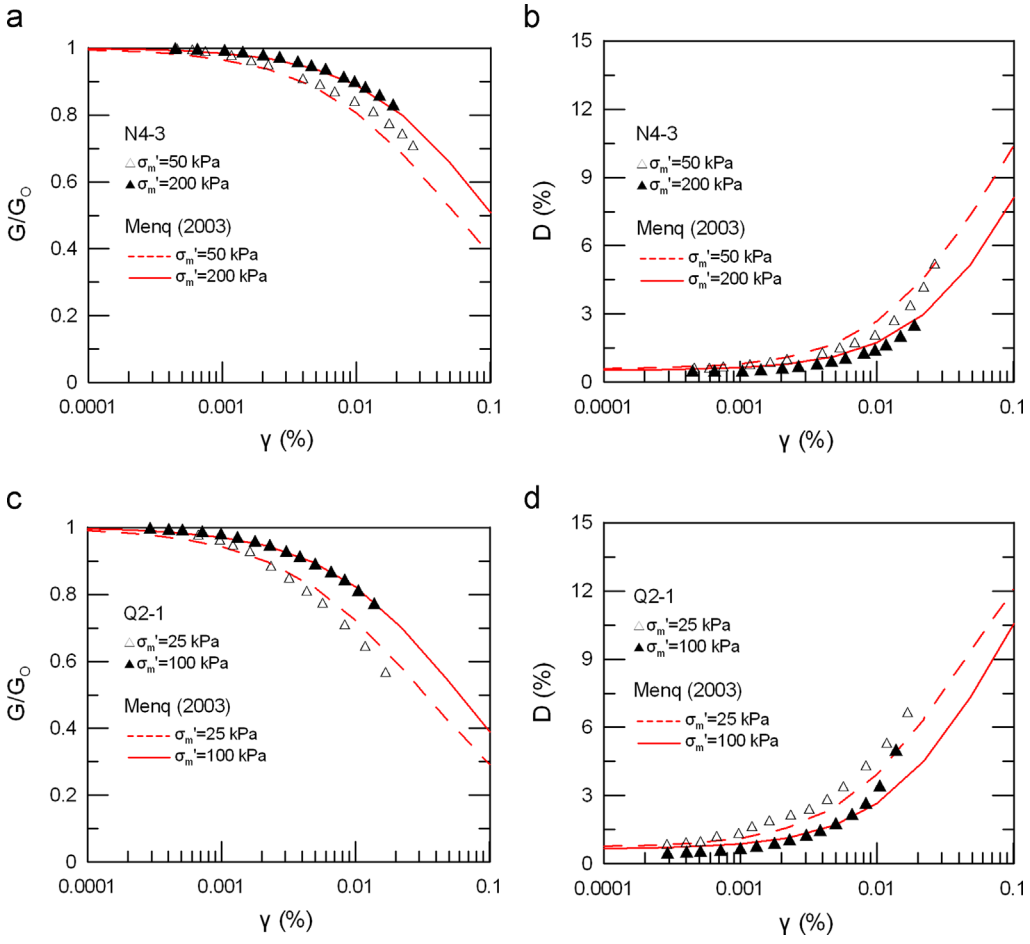

Fig. 2. Experimentally against analytically derived G/G_O-log γ and D-log γ curves of quartz sands of this study: representative results.

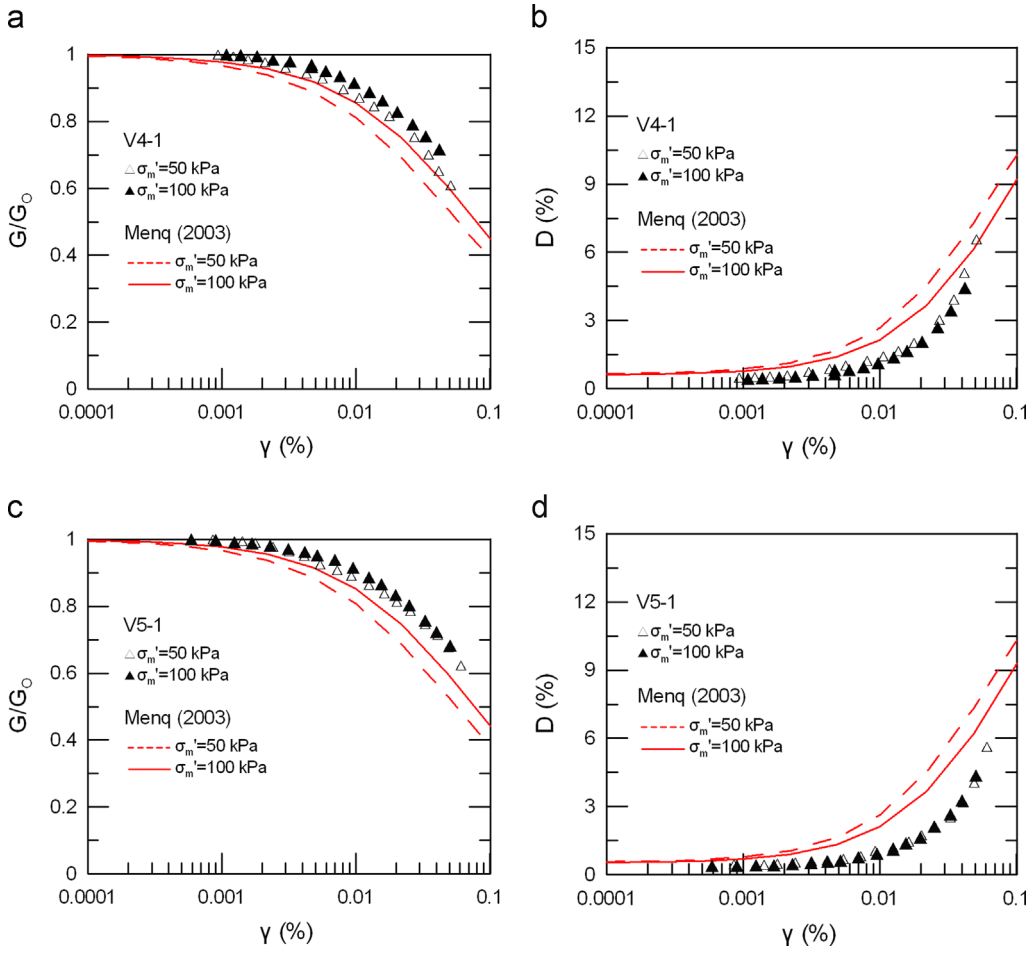

Fig. 3. Experimentally against analytically derived G/G_O-log γ and D-log γ curves of volcanic sands of this study: *R*epresentative results.

the expression $0.12 \times C_u^{-0.6}$, while the exponent n_γ may be estimated through the expression $0.5 \times C_u^{-0.15}$. It is also noted that in Eq. (2), the reference strain is expressed in percentile scale.

$$\frac{G}{G_O} = \frac{1}{1+(\gamma/\gamma_{\text{ref}})^a} \tag{1}$$

$$\gamma_{\text{ref}} = A_\gamma \left(\frac{\sigma_m'}{P_a}\right)^{n_\gamma} \tag{2}$$

$$a = 0.86 + 0.1 \times \log\left(\frac{\sigma_m'}{P_a}\right) \tag{3}$$

The expression for the material damping, denoted as D_{Masing}, using the Masing model is shown in Eq. (4). Darendeli (2001) proposed the correction of this model in two steps; first, a correction of the damping ratio derived from Eq. (4) is implemented through Eq. (5), denoted as D_{correct}, in order to predict the damping of soils at relatively large strains in a more realistic manner, and then the damping ratio of Eq. (5) is normalized with respect to the small-strain damping, D_O, through Eq. (6). In Eq. (5), the constants c_1, c_2 and c_3 depend on the curvature coefficient, given in Eq. (3) for granular soils, while parameter b of Eq. (6) is used in order to account the effect of the number of loading cycles on damping ratio. Details of these relationships have been presented elsewhere (Darendeli, 2001; Menq, 2003). In Eqs. (4)–(6), the damping ratio is given in percentile scale.

$$D_{\text{Masing}} = \frac{100}{\pi}\left[4 \times \frac{\gamma - \gamma_{\text{ref}} \ln((\gamma+\gamma_{\text{ref}})/\gamma_{\text{ref}})}{(\gamma^2/(\gamma+\gamma_{\text{ref}}))} - 2\right] \tag{4}$$

$$D_{\text{correct}} = c_1 D_{\text{Masing}} + c_2 D_{\text{Masing}}^2 + c_3 D_{\text{Masing}}^3 \tag{5}$$

$$D - D_O = b\left(\frac{G}{G_0}\right)^{0.1} \times D_{\text{correct}} \tag{6}$$

Thereupon, each theoretical curve of Figs. 2 and 3 concerns the specific C_u value of each specimen (given in Table 1) as well as the specific σ_m' magnitude where each specimen was tested (illustrated in Figs. 2 and 3). For the estimated damping ratio values in these figures, a spectrum of number of loading cycles that represent the RC experiments were used. The typical range of the number of loading cycles during the RC tests for quartz and volcanic sands are presented briefly in Section 4.

As shown in Fig. 2, the analytical relationships proposed by Menq (2003) satisfactorily predict the response of specimens N4-3 and Q2-1. However, as shown in Fig. 3, the volcanic

sands exhibit systematically more linear shape of the G/G_O-log γ and D-log γ curves in comparison to the theoretical ones. This non-satisfactory convergence between the G/G_O-log γ and D-log γ curves of specimens V4-1 and V5-1 and the theoretical curves proposed by Menq (2003) was observed in all the volcanic sands of this study.

In Fig. 4a and b we plot the measured G/G_O and D values against the shear strain amplitude of all the quartz sands and in Fig. 4c and d we do the same for the volcanic soils. In general, no significant effect of particles shape, in terms of roundness, on the G/G_O-log γ and D-log γ curves of the quartz sands was observed, and thus, the experimental results of the sub-rounded to rounded and sub-angular to angular quartz sands are plotted in the same figure. In addition, no monotonic trend of the effect of void ratio (or relative density) on the G/G_O-log γ and D-log γ curves was observed in either the quartz and the volcanic sands, which is in agreement with the available data presented in the literature (e.g., Kokusho, 1980; Menq, 2003).

In Fig. 4 we also plot a spectrum of G/G_O-log γ and D-log γ curves derived from the analytical relationships proposed by Menq (2003) for granular soils as presented in Eqs. (1)–(6). According to these equations, the G/G_O-log γ and D-log γ curves of granular soils exhibit more linear shape as σ'_m increases and C_u decreases. Thereafter, we decided to use an upper bound for the theoretical G/G_O-log γ curves plotted in Fig. 4 (as well as a respective lower bound for the D-log γ curves) that corresponds to the lower C_u values of the materials under study, equal to 1.3 for the quartz and 1.5 for the volcanic sands, and to the higher σ'_m where HARCT were performed, equal to 200 kPa. The lower bound for the theoretical G/G_O-log γ curves of Fig. 4 (as well as the respective higher bound for the D-log γ curves) corresponds to the higher C_u values of the materials under study, equal to 3.2 for the quartz and 4.2 for the volcanic sands, and the lower σ'_m where HARCT were performed, equal to 25 kPa.

With respect to the quartz sands, it is observed in Fig. 4a and b that the measured G/G_O and D values are plotted, in general, within the lower–upper bounds of the analytically derived curves. The variability of the G/G_O and D values of the quartz sands at a given shear strain amplitude is attributed, primarily, to the variability of the mean effective confining pressure (σ'_m), as also depicted in Fig. 2 with an additional effect of the coefficient of uniformity (C_u) and the mean grain size (d_{50}). With respect to the volcanic sands, it is interesting to note in Fig. 4c and d that all the measured G/G_O values are located at the upper bound, whereas the D values are located at

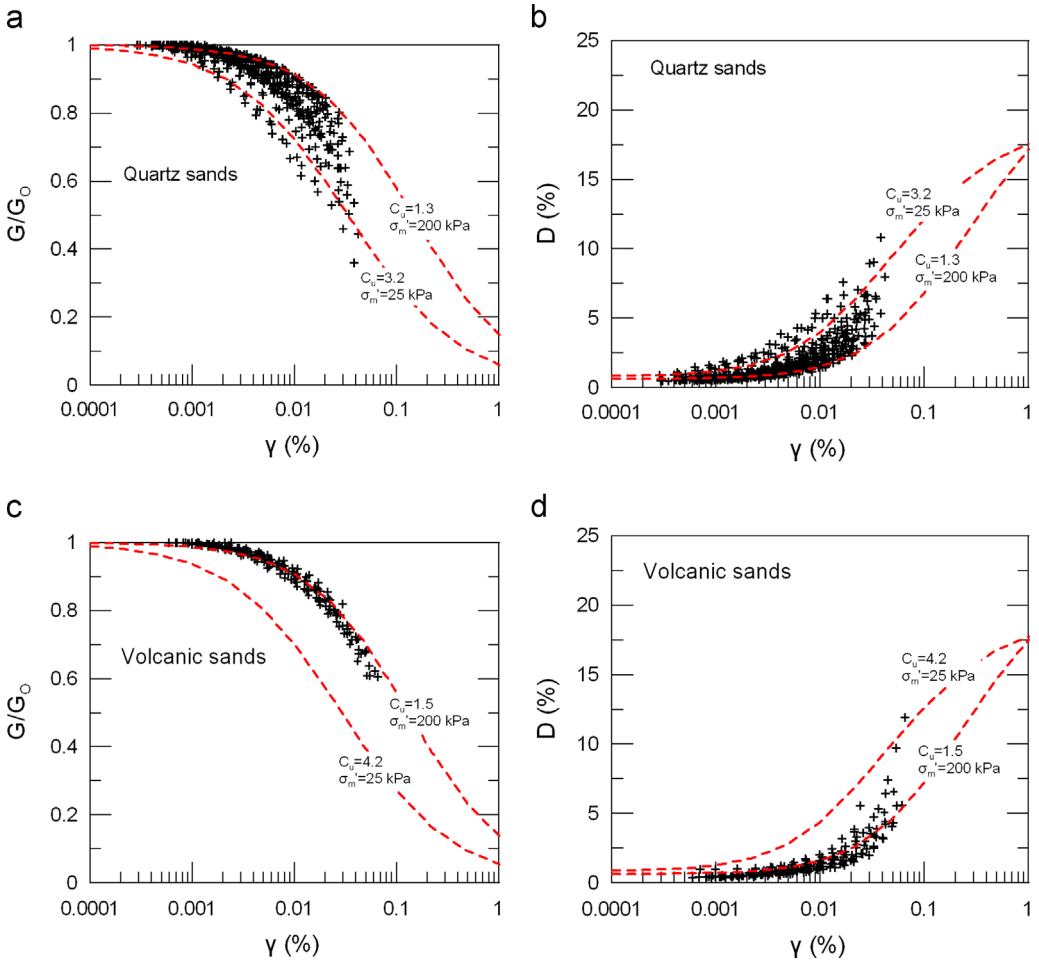

Fig. 4. G/G_O and D values against the shear strain amplitude: (a), (b) quartz sands and (c) and (d) volcanic sands along with upper-lower bounds proposed by Menq (2003).

the lower bound of the literature curves. As is also illustrated in Fig. 3, this is partially attributed to the higher linearity that the volcanic sands exhibit in the range of medium shear strain levels in comparison to the quartz sands. Although the volcanic sands of this study had variable grain size distribution and the specimens were tested at elevated confining pressures such as the quartz soils, the variability of the G/G_O and D values of Fig. 4c and d at a given shear strain amplitude is less pronounced in comparison to Fig. 4a and b. It seems therefore that parameters such as the mean effective confining pressure σ'_m along with the grain-size characteristics, that have been used in previous studies efficiently in order to quantify the rate of modulus decrease and damping increase in quartz soils, might not be such strong parameters in crushable soils, as shown by the volcanic sands used in this study. This assertion is supported by Anastasiadis et al. (2010), Senetakis (2011) and Senetakis et al. (2013a) who studied the dynamic properties of the coarse fractions of a pumice soil (artificially crushed rock), which has different physical properties and compaction characteristics in comparison to the volcanic sands of this paper.

3.2. Analysis of experimental HARCT results

3.2.1. G/G_O-log γ curves

According to the RC test results and after analyzing the normalized modulus degradation curves through the modified hyperbolic model, no strong effect of σ'_m, particle distribution, shape and mineralogy was observed on the curvature coefficient (a). The "experimentally" derived curvature coefficient values of all specimens are summarized in Table 2. Parameter (a) ranged from 0.85 to 1.14 with an average value equal to 1.00 and a value of the standard deviation equal to 0.06. Thereupon, the modified hyperbolic model of Eq. (1) is transformed to Eq. (7).

$$\frac{G}{G_O} = \frac{1}{1+(\gamma/\gamma_{ref})} \tag{7}$$

In Fig. 5 we plot the "experimentally" derived A_γ values separately for the quartz and the volcanic sands, against the coefficient of uniformity (C_u) and the mean grain size of particles (d_{50}). These values are also summarized in Table 2. With reference to the quartz sands (Fig. 5a and b) it is shown that there is a general trend of decreasing A_γ with increasing C_u and d_{50}, but the data are scattered as also implied by the relatively low values of the coefficients of correlation R^2. This slight trend of decreasing A_γ implies that γ_{ref} decreases and thus, the sands exhibit higher non-linearity in the range of medium to high strain levels with increasing C_u and d_{50}. However, it is noted in Fig. 5a and b that a slightly better correlation may be found between A_γ and C_u than A_γ and d_{50} with respect to the R^2 values. Therefore, the reference strain of the quartz sands was expressed analytically as a function of C_u and not d_{50}. In Fig. 5c and d, it can be seen that the parameters C_u and d_{50} do not affect in a monotonic way the reference strain of the volcanic sands, and thus, for these soils we decided to use an average value of the reference strain, also depicted in the aforementioned figures.

Table 2
Reference strain parameters (A_γ, n_γ) and curvature coefficient values (a) of sandy specimens of this study.

Code name of specimen	e_o	A_γ (%)	n_γ	(a) Values at variable σ'_m (kPa)			
				25	50	100	200
(1)	(2)	(3)	(4)	(5)	(6)	(7)	(8)
N1-1	0.661	0.088	0.48	–	0.95	0.95	0.95
N1-2	0.964	0.080	0.46	–	–	1.00	1.01
N2-3	0.588	0.070	0.42	1.03	0.97	0.97	0.95
N2-4	0.682	0.056	0.36	1.12	1.08	0.99	–
N3-1	0.680	0.095	0.21	–	–	0.98	0.98
N3-2	0.938	0.089	0.31	–	–	1.05	1.00
N4-2	0.571	0.096	0.26	–	–	0.92	0.97
N4-3	0.588	0.085	0.18	–	0.85	0.93	1.00
Q1-1	0.683	0.062	0.67	–	0.92	0.99	1.03
Q1-2	0.954	0.075	0.56	–	0.99	1.02	–
Q2-1	0.545	0.042	0.46	0.95	–	1.02	1.02
Q3-1	0.594	0.042	0.58	1.00	–	1.00	1.02
Q3-2	0.820	0.052[a]	0.03[a]	–	–	0.99	1.06
Q4-1	0.553	0.035	0.49	1.04	0.97	1.05	–
Q4-2	0.770	0.044	0.48	0.98	0.99	0.98	–
V1-1	0.823	0.086	0.04	–	1.02	1.04	1.10
V2-1	0.961	0.105	0.11	1.01	–	1.03	–
V2-2	1.250	0.132	0.20	0.96	–	1.04	–
V3-2	0.898	0.085	0.05	–	–	1.07	1.14
V4-1	0.943	0.097	0.04	–	0.97	1.02	–
V5-1	0.976	0.115	0.06	–	0.87	0.96	–

[a]Not included in the regression analysis.

The n_γ values of all specimens are summarized in Table 2. The quartz sands had n_γ values ranging from 0.18 to 0.67 with an average value equal to 0.42, while the volcanic soils showed remarkably lower n_γ values ranging from 0.04 to 0.20, with an average value equal to 0.08. Consequently, the overall effect of σ'_m on the normalized modulus degradation and damping ratio increase in the range of medium shear strains is very small for the volcanic sands.

According to the experimental results presented in Fig. 5 and Table 2, the reference strain (γ_{ref}) of the materials under study may be expressed as a function of mean effective confining pressure through Eqs. (8a) and (8b), separately for quartz and volcanic sands. We note that γ_{ref} is given in percentile scale (%) and e corresponds to the Napierian logarithm.

$$\text{Quartz sands}: \ \gamma_{ref} = 0.159 \times e^{-0.419 \times C_u} \times \left(\frac{\sigma'_m}{P_a}\right)^{0.42} \tag{8a}$$

$$\text{Volcanic sands}: \ \gamma_{ref} = 0.100 \left(\frac{\sigma'_m}{P_a}\right)^{0.08} \tag{8b}$$

3.2.2. D-log γ curves

In Fig. 6a we plot the damping ratio values, expressed as $D-D_O$, against the corresponding G/G_O values of all specimens, where D_O is the small-strain damping. In particular, there no clear trend observed of the effect of particles

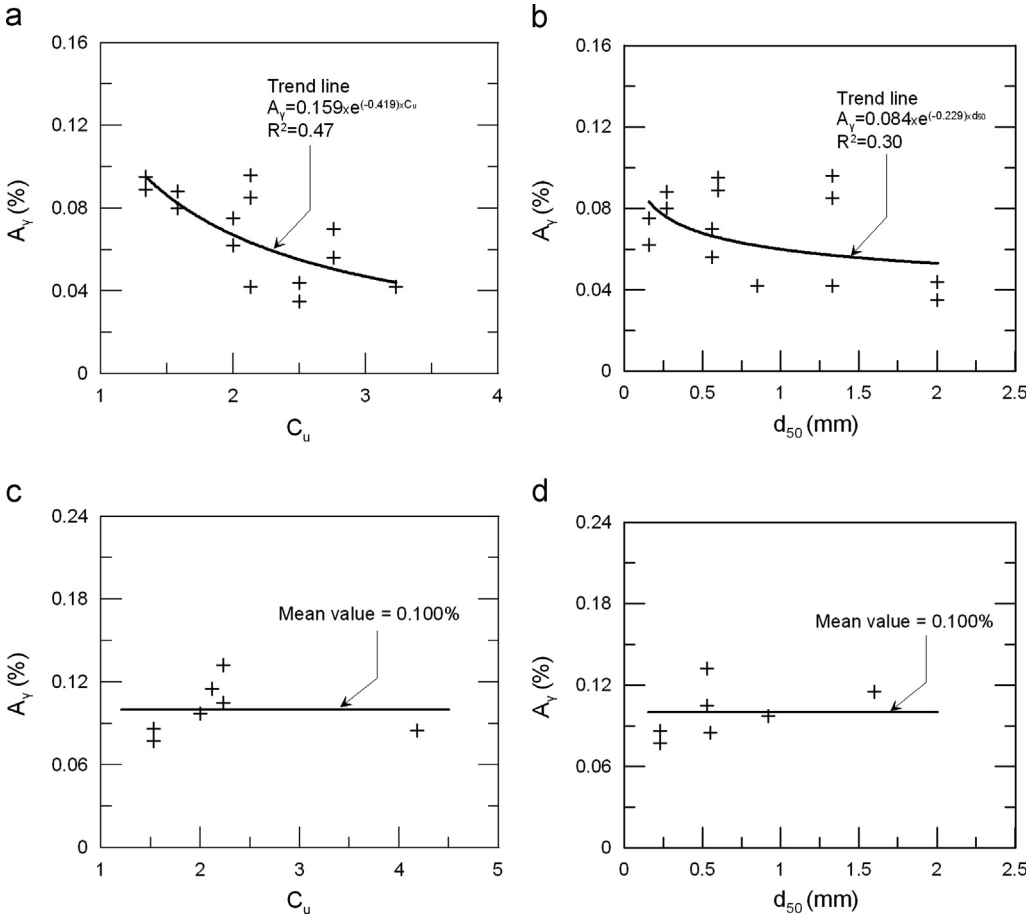

Fig. 5. Effect of coefficient of uniformity C_u and mean grain size d_{50} on the parameter A_γ of: (a), (b) quartz sands and (c) and (d) volcanic sands.

distribution, shape and mineralogy on the correlation between the measured $D-D_O$ and G/G_O values, and thus, we decided to use an average two-order polynomial curve for all specimens, also illustrated in Fig. 6a. The general form of this equation is given analytically in Eq. (9), where a_1, a_2 and a_3 are the fitting parameters. This equation has been also used in the past in other studies in order to correlate the damping increase with the degradation of the normalized modulus of granular and cohesive soils (e.g., Zhang et al., 2005).

$$D-D_O(\%)=a_1\left(\frac{G}{G_O}\right)^2+a_2\left(\frac{G}{G_O}\right)+a_3 \tag{9}$$

In Fig. 6b we compare the fitting curve of this study with other curves proposed in the literature. Considering the experimental results of Fig. 6, Eq. (9) may be transmitted to Eq. (10), where $D-D_O$ is given in percentile scale (%). Expressions for the small-strain damping ratio, D_O, for the sands of this study have been presented by Senetakis et al. (2012a).

$$D-D_O(\%)=7.22\times\left(\frac{G}{G_O}\right)^2-25.25\times\left(\frac{G}{G_O}\right)+17.96 \tag{10}$$

3.2.3. Measured against estimated G/G_O and $D-D_O$ values of this study

Using Eqs. (7)–(10), in Fig. 7 we plot the measured against the analytically derived G/G_O and $D-D_O$ values of this study. Considering the general complexity in studying the dynamic response of particulate materials at medium to high shear strain levels, which complexity is more pronounced for the damping ratio in shear, the comparison between measured and estimated G/G_O and $D-D_O$ in Fig. 7 is satisfactory for practical geotechnical purposes.

3.3. Design G/G_O-log γ and D-log γ curves for quartz and volcanic sands

Using the analytical relationships developed on the framework of this paper, in Figs. 8 and 9 we present design G/G_O-log γ and D-log γ curves for quartz and volcanic poor-graded sands of C_u=1.5, at elevated mean effective confining pressures. In the same figures we plot the corresponding curves proposed by Menq (2003) for sandy soils (using the same value of C_u). As expected, the design curves proposed for quartz sands (Fig. 8) are in good agreement with the corresponding curves proposed by Menq (2003). However, the following should be noted for Fig. 9: (1) The design curves for the volcanic sands at $\sigma'_m=25$ kPa are significantly more linear in shape in comparison to the corresponding literature curves. (2) The design curves for the volcanic sands at $\sigma'_m=100$ kPa are in good agreement with the corresponding literature curves. (3) The effect of σ'_m on the rate of modulus degradation and damping increase of the volcanic sands of this

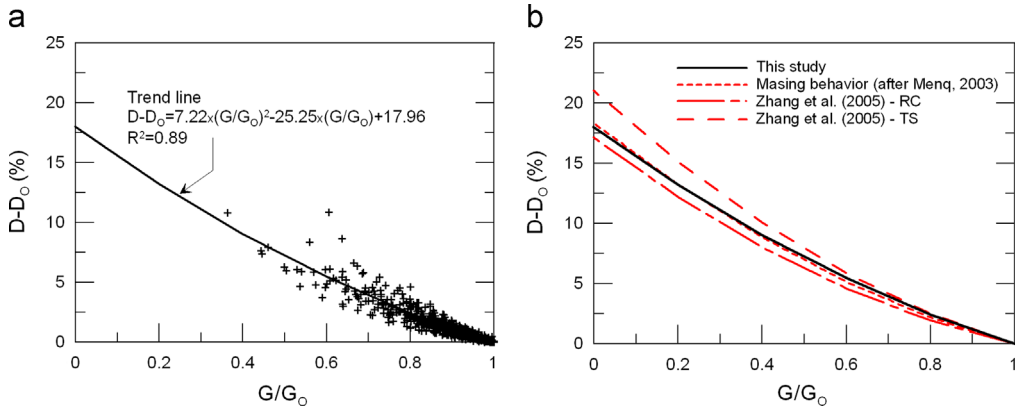

Fig. 6. Damping ratio $D-D_O$ against G/G_O (a) experimental results and corresponding fitting curve of this study and (b) comparison with curves proposed in the literature.

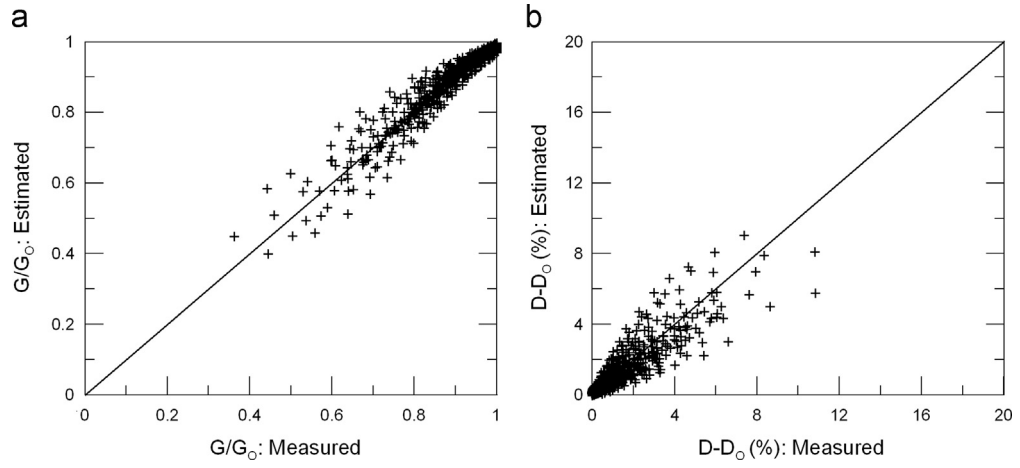

Fig. 7. Experimentally against analytically derived values of normalized shear modulus, G/G_O, and damping ratio expressed as $D-D_O$ of sandy specimens of this study.

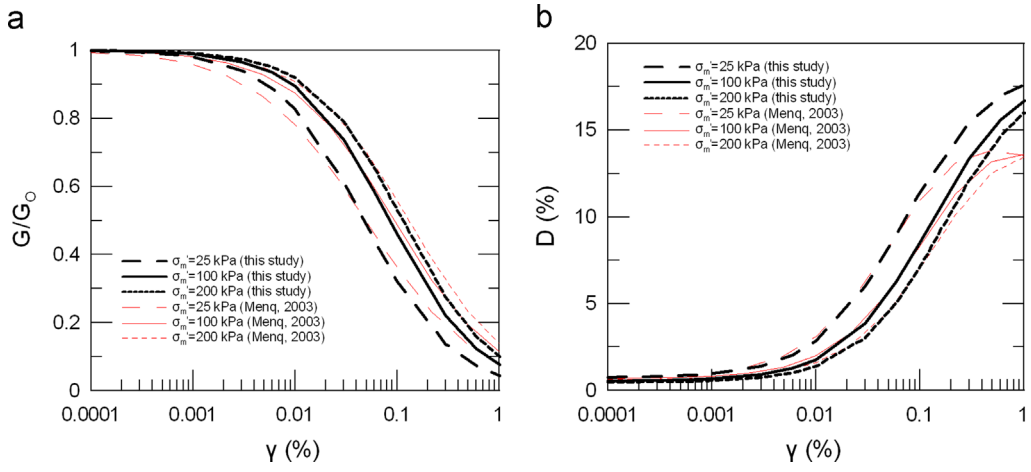

Fig. 8. Design G/G_O-log γ and D-log γ curves for quartz sands $C_u=1.5$ proposed in this study and comparison with corresponding curves proposed by Menq (2003).

study is very small. Therefore, it is concluded that the available curves proposed in the literature for typical sands predominately composed of quartz particles do not satisfactorily represent the behavior of volcanic soils which have been characterized by other researchers as "non-textbook" geomaterials, and that the confining pressure and the coefficient of uniformity may not be useful parameters when quantifying and predicting the rate of modulus degradation and damping increase with increasing shear strain in crushable soils such as the volcanic sands of this study.

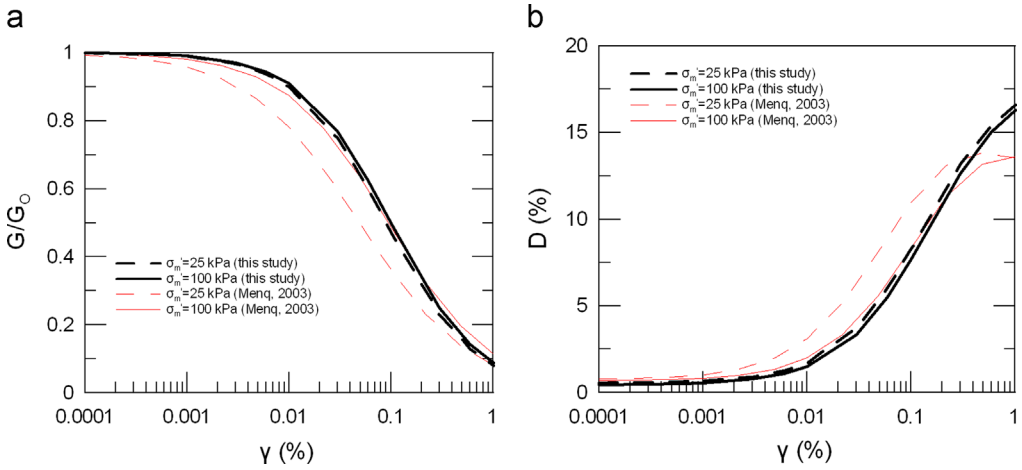

Fig. 9. Design G/G_O-log γ and D-log γ curves for volcanic sands of $C_u=1.5$ proposed in this study and comparison with corresponding curves proposed by Menq (2003).

In Fig. 10 we compare the design curves of this study between quartz and volcanic sands of $C_u=1.5$, at variable mean effective confining pressures. As mentioned previously, the volcanic sands exhibit significantly more linear behavior at low confining pressures ($\sigma'_m=25$ kPa) in comparison to the quartz granular soils. However, due to the relatively negligible effect of σ'_m on the rate of modulus degradation and damping increase in the volcanic soils, it is observed that at higher confining pressures quartz and volcanic sands of $C_u=1.5$ exhibit similar G/G_O-log γ and D-log curves.

Finally, in Fig. 11 we compare the design curves of this study between quartz and volcanic sands of $C_u=3.0$, at variable mean effective confining pressures. One of the most important findings of this research work was that the increase of the coefficient of uniformity, C_u, does not reflect a more pronounced non-linear response of the volcanic granular soils which was in contrast with the data on quartz sands of strong particles. Consequently, the design curves of the volcanic sands in Fig. 11 are very similar to the corresponding curves of Fig. 10, whereas, for the quartz sands, the curves of Fig. 11 with $C_u=3.0$ have steeper shape in comparison to the curves of Fig. 10 with $C_u=1.5$. It is concluded, in contrast to Fig. 10, that for a coefficient of uniformity equal to 3.00, the volcanic sands exhibit significantly more linear shape of the G/G_O-log γ and D-log γ curves in comparison to the quartz sands, whatever the mean effective confining pressure.

4. Discussion

Due to the well-known restrictions of the resonant column testing, we were not able to control the number of the imposed loading cycles on the specimens during the performance of the HARCT. One could expect that the observed more linear shape of the G/G_O-log γ and D-log γ curves of the volcanic sands in comparison to the quartz ones is somehow related to the effect of the number of loading cycles, N. In general, the imposed number of loading cycles (N) to the quartz samples at each step of RC measurements and assuming an elapsed time of 30 s during the RC records at a given shear strain amplitude ranged between 1500 and 6000 cycles, approximately, depending on sample density, the confining pressure and the shear strain amplitude. In the volcanic sands which soils have much lower values of the small-strain stiffness (Senetakis et al., 2012a), the resonant frequencies at which the RC data were obtained were much lower in comparison to the quartz sands with a corresponding lower imposed number of loading cycles ranging between 900 and 3500 approximately. However, in the literature it has been reported that the increase of N tends to lead to smoother curves, whereas for a total number of imposed loading cycles above 10, the overall effect of N on the G/G_O-log γ and D-log γ curves of dry sands is not that important (e.g., Stokoe et al., 1994; Ishihara, 1996). As such, we cannot strongly correlate the effect of N with the observed more linear behavior of the volcanic sands in comparison to the quartz ones.

At a given shear strain amplitude and mean effective confining pressure, we could partially correlate the more linear shape of the G/G_O-log γ curves of the volcanic sands in comparison to the quartz sands with the different micro-mechanical properties and dominant micro-mechanisms between materials of variable types. For example, it has been shown from numerical studies using the discrete element method that different friction angles at the contacts of soil particles may lead to different responses on the macro-scale level in both monotonic (e.g., Thornton, 2000; Barreto and O' Sullivan, 2012) and cyclic loading (e.g., Sazzad and Suzuki, 2011). In addition, Cole and Peters (2008) and Senetakis et al. (2013b) have shown through micro-mechanical experiments that along with the effect of mineral type on the frictional response and frictional losses at the particle contacts, there is an additional effect of particle type on the inter-particle stiffness in both the normal and tangential directions with higher stiffness at the contacts of stronger particles in comparison to softer ones. These differences in stiffness will also affect the resultant macro-scale deformations into the soil mass during dynamic loading, depending on the type of particles. While in the studies by Senetakis et al. (2013b, 2013c) it has been shown that for quartz particles the steady state sliding is in general observed at extremely small displacements, less than 1 μm in most experiments, for weak-crushable particles of limestone, Senetakis

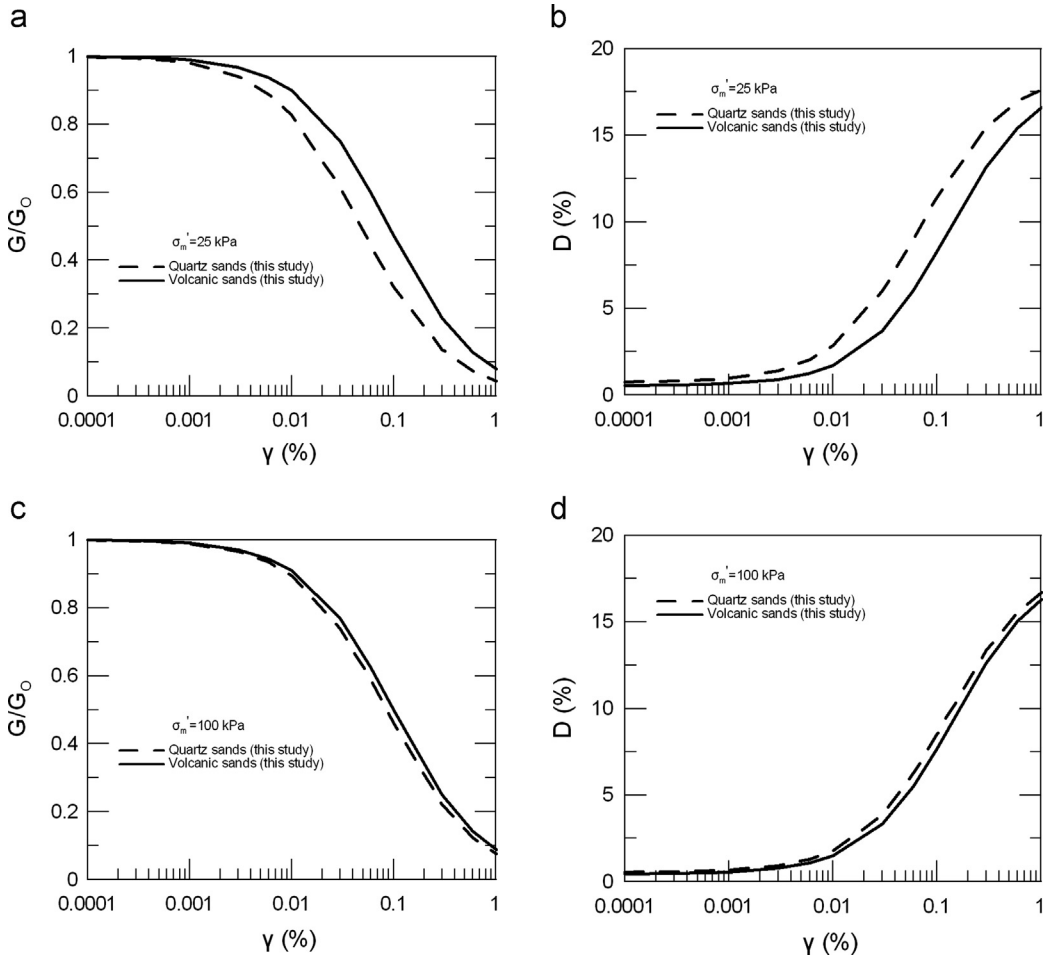

Fig. 10. Comparison between design G/G_O-log γ and D-log γ curves for quartz and volcanic ($C_u=1.5$) sands of this study at variable mean effective confining pressures.

et al. (2013b) showed that the overall steady state sliding at the contacts of the particles and the mobilization of the dynamic coefficient of friction tends to shift to larger strains. These findings imply that the changes in soil fabric through re-arrangement of the particles and changes in coordination number may be affected by the type of material, with different energy dissipation mechanisms between the assemblies of strong and weak-crushable particles. In the quartz assemblies, slippage and re-arrangement of particles take place after a very small amount of micro-slip at particle contacts and this mechanism may play an important role in the dissipation of energy in the soil mass, followed by a more abrupt increase of damping and decrease of the normalized modulus during shearing. In the weak volcanic assemblies, and at least at in the early stages of increasing shear strain, the energy is possibly dissipated, primarily, through damage to the asperities (as also reported by Senetakis et al., 2013a in other volcanic soils) and an increase in force is necessary to mobilize the dynamic friction at particle contacts. It may then be assumed that micro-mechanisms prevail in these sands while the energy dissipation in the quartz might be more global through slippage and changes in fabric on the macro-scale level. These considerations may be also related to the observed more pronounced changes of sample height during torsional loading in the quartz sands recorded by a vertically position displacement transducer, while in the volcanic sands the overall changes of sample height were less important during HARCT.

It is a general perception that for a given material type the geometry and morphology of the particles including particle size, size distribution, shape descriptors, surface roughness and intra-particle voids play an important role in the micro-mechanical properties of soil particles at their contacts and that these affect the overall macro-scale response of the granular assembly (e.g., Santamarina and Cascante, 1996, 1998; Yimsiri and Soga, 2000; Cho et al., 2006; Sezer et al., 2011; Senetakis et al., 2012a, 2013a). In the micro-mechanical experiments by Senetakis et al. (2013b) it was demonstrated that the hardness of material may very well be a key factor in the monotonic and cyclic response of sands on the micro-scale level. For example, the more pronounced damage of the asperities during the torsional loading at the contacts of weak volcanic particles of lower hardness in comparison to strong quartz particles of higher hardness may lead to a different evolution in the re-arrangement of particles and fabric changes between volcanic and quartz granular assemblies along with different energy losses at the particle contacts. These different responses may result in different energy

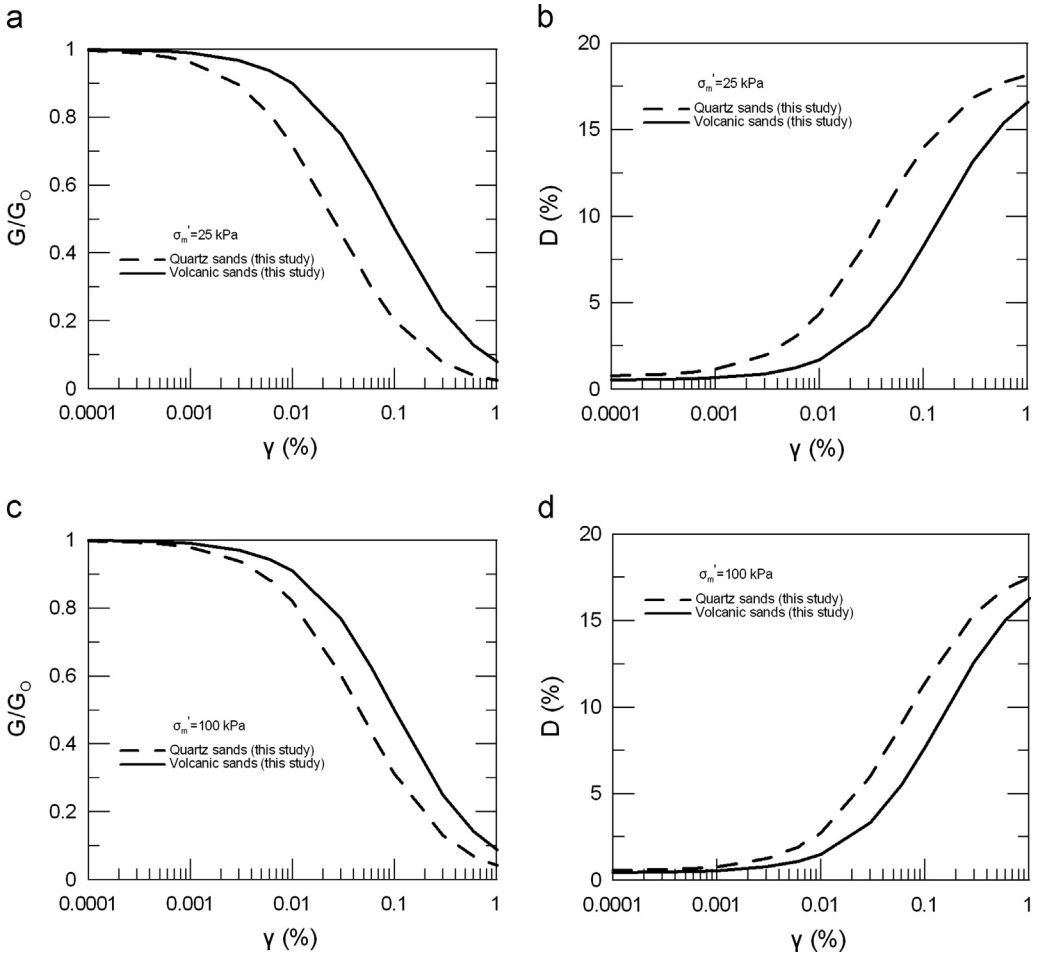

Fig. 11. Comparison between design G/G_O-log γ and D-log γ curves for quartz and volcanic sands (C_u=3.0) of this study at variable mean effective confining pressures.

dissipation mechanisms since the fabric changes will promote the dissipation of energy through inter-particle friction (Wang and Yan, 2013, 2012). Considering this, it is possible that the more pronounced dissipated energy at the contacts of volcanic particles along with particle re-arrangement and resultant new particle contacts development in the volcanic assemblies may lead to an overall less pronounced macro-scale damping increase in the rhyolitic crushed rock in comparison to the quartz samples. This lower rate of damping increase will result in less pronounced modulus degradation in the volcanic assemblies in comparison to the quartz ones and this may explain, partially, the more linear response observed in the volcanic samples. The latter remark was also supported in studies on other crushable soils such as pumice gravel tested by Senetakis et al. (2013a). In that study, Senetakis et al. also observed more linear response of the pumice soil in comparison to quartz of similar grading characteristics.

On the other hand, it is possible that changes in the confining pressure will result in more pronounced fabric changes and damage to the surface geometry in the weak volcanic sands than in strong quartz during the elevation of σ_m′. This assumption was supported by the more pronounced changes in the sample height in the weak volcanic assemblies than in quartz ones during the increase of the mean effective confining pressure. The more pronounced fabric changes in the weak volcanic samples during the elevation of σ'_m and before the torsional loading along with more pronounced damage of the surface characteristics in the volcanic particles than in quartz ones will possibly lead to an alteration of the prevailed energy dissipation mechanisms in the volcanic soils when σ'_m is increased. In the volcanic sands and at lower σ'_m, it may well be that the energy is dissipated through the micro-mechanisms mentioned above, while at higher pressures and due to the more pronounced changes in soil fabric, the slippage at particle contacts becomes more pronounced during shearing and at the same level of the shear strain which reflects a more global dissipation of energy such as in the quartz samples. The latter remark implies that in the quartz and because of the small effect of the confinement on the fabric changes, energy dissipation occurs because of similar mechanisms for the range of σ'_m of this study. This reflects the clear effect σ'_m on the modulus degradation and damping increase in the quartz samples. In contrast, in the crushable volcanic particles, the mechanisms of energy dissipation may be altered as σ'_m increases, which implies that σ'_m may not be a useful parameter in predicting the G/G_O-log γ and D-log γ curves in these sands.

The above micro-mechanical considerations should be further examined, for example, through examination of the changes in the surface characteristics of the soil particles because of the torsional loading, or micro-mechanical inter-particle shearing tests that would possibly lead to a better understanding of the different energy losses at the contacts of quartz–quartz and volcanic–volcanic particles. In this study, only macro-scale experiments were conducted, while the possible effect of the response at the contacts of the particles on the macro-scale response of the samples was only examined through sieving analysis tests before and after the performance of the RC experiments. These tests showed that while no significant change was observed in the grading of the volcanic samples after the performance of the RC experiments, a small amount of finer particles was produced in these samples possibly due to the coupled effect of the elevation of the isotropic pressure and the dynamic loading. This small amount of finer particles found in the volcanic samples indicates that crushing affects the dissipation of energy in these crushable soils, while in the quartz samples of strong particles the energy dissipation is more global through particle re-arrangement during the dynamic loading. It is a general perception that the crushing of particles plays an important role in the overall mechanical response of particulate media (e.g., Coop, 1990; Coop et al., 2004; Lobo-Guerrero and Vallejo, 2005, 2006; Yao et al., 2008; Vilhar et al., 2013) but most studies have been focused on the breakage of particles associated with large strains where the soils deform under a constant volume. However, the findings of this experimental work indicate that particle crushing or crushing of the asperities even on the micro-scale level may promote very important energy dissipation mechanisms resulting in a reduction of the rate of modulus degradation and increase in material damping even at relatively small to medium shear strain amplitudes.

5. Conclusions

We presented a synthesis of high-amplitude torsional resonant column test results on dry specimens of quartz sand of strong particles and volcanic sands composed of rhyolitic crushed rock of crushable particles of intra-particle voids. In order to quantitatively identify the possible differences between quartz and volcanic sands at a macro-scale level as well as to extrapolate the experimental data to higher shear strain levels and propose useful data for current engineering practice, we implemented the well-known modified hyperbolic model for the analysis of the G/G_O-log γ curves, whilst the D-log γ curves were analyzed by correlating the damping increase with the modulus degradation through a simple two-order polynomial relationship.

The G/G_O-log γ and D-log γ curves of the volcanic sands were systematically more linear than those of the quartz ones. This trend was more pronounced at lower levels of the mean effective confining pressure (σ'_m) and at higher values of the coefficient of uniformity (C_u). These differences in the observed responses between quartz and volcanic sands were attributed, partially, to the different mechanisms on a micro-scale level that dominate in granular assemblies of variable particle types along with differences in the morphological and surface characteristics of the particles.

Because of the possible more pronounce crushing of the asperities of the volcanic particles along with different harnesses, friction angle values and stiffnesses at particle contacts between quartz and volcanic sands, the energy is dissipated primarily because of deformations and damage of the surface characteristics at particle contacts in the volcanic sands. In the quartz sands of strong particles, the steady state sliding at particle contacts and global slippage take place at smaller deformations and thus, in the quartz sands the more pronounced damping increase and stiffness degradation in comparison to the volcanic sands was, primarily, because of the more pronounced global slippage and fabric changes during the torsional loading. This was also verified by the more pronounced changes in sample height during the dynamic loading that was observed in the quartz sands. In contrast, after the high-amplitude RC tests, a small amount of finer particles was produced in the volcanic sands, indicating that the energy dissipation mechanisms in these sands of weak particles differed from those of the quartz assemblies of strong particles.

In contrast to the quartz sands, parameters such as the mean effective confining pressure (σ'_m) and the coefficient of uniformity (C_u) could not be efficiently used in the modified hyperbolic model to quantify the rate of modulus degradation and increase in damping in the volcanic sands. This may be because the more pronounced fabric changes in the volcanic assembles during the elevation of the mean effective confinement led to the alteration of the prevailing energy dissipation mechanisms in these soils, whereas the relatively more stable fabric of the quartz assembly led to similar energy dissipation mechanisms regardless of the confining pressure.

Acknowledgments

The anonymous reviewers are acknowledged for their constructive comments that helped us to improve the quality of the paper. The work described in this paper was partially supported by a Grant from the Research Grants Council of the Hong Kong Special Administrative Region China (Project no. CityU112911).

References

Aggur, M., Zhang, J., 2006. Degradation of sands due to combined sinusoidal loading. J. Geotech. Geoenviron. Eng., ASCE 132 (12), 1628–1632.

Anderson D., 1974. Dynamic Modulus of Cohesive Soils (Ph.D. dissertation). University of Michigan, USA.

Anastasiadis A., Senetakis K. and Pitilakis K., 2010. Dynamic properties of volcanic granular soils. In: Proceedings of the 6th Hellenic Conference on Geotechnical and Geo-environmental Engineering, Volos, Greece (in Greek).

Anastasiadis A., Pitilakis K., Senetakis K. and Souli A., 2011. Dynamic response of sandy and gravelly soils: effect of grain size characteristics on G-γ-D curves. In: Proceedings of the 5th International Conference on Earthquake Geotechnical Engineering, January 10–13, Santiago, Chile.

Anastasiadis, A., Senetakis, K., Pitilakis, K., Gargala, C., Karakasi, I., 2012. Dynamic behavior of sand/rubber mixtures, Part I: effect of rubber content and duration of confinement on small-strain shear modulus and damping ratio. J. ASTM Int. 9 (2), 03680 (Paper ID JAI1).

ASTM, 1992. Standard test methods for modulus and damping of soils by the resonant column method: D4015-92. Annual Book of ASTM Standards, ASTM International.

Barreto, D., O' Sullivan, C., 2012. The influence of inter-particle friction and the intermediate stress ratio on soil response under generalised stress conditions. Granular Matter 14, 505–521.

Cho, G.-C., Dodds, J., Santamarina, C., 2006. Particle shape on packing density, stiffness, and strength. J. Geotech. Geoenviron. Eng., ASCE 132 (5), 591–602.

Cole, D.M., Peters, J.F., 2008. Grain-scale mechanics of geologic materials and lunar simulants under normal loading. Granular Matter 10, 171–185.

Coop, M., 1990. The mechanics of uncemented carbonate sands. Géotechnique 40 (4), 607–626.

Coop, M., Sorensen, K., Bodas Freitas, T., Georgoutsos, G., 2004. Particle breakage during shearing of a carbonate sand. Géotechnique 54 (3), 157–163.

Darendeli M., 1997. Dynamic Properties of Soils Subjected to 1994 Northridge Earthquake (M.S. dissertation). University of Texas at Austin, USA.

Darendeli M., 2001. Development of a New Family of Normalized Modulus Reduction and Material Damping Curves (Ph.D. dissertation). University of Texas at Austin, USA.

Drnevich V., 1967. Effects of Strain History on the Dynamic Properties of Sand (Ph.D. dissertation). University of Michigan, USA.

Hardin, B., Drnevich, V., 1972a. Shear modulus and damping in soils: Measurement and parameter effects. J. Soil Mech. Found., ASCE 18 (SM6), 603–624.

Hardin, B., Drnevich, V., 1972b. Shear modulus and damping in soils: Design equations and curves. J. Soil Mech. Found., ASCE 98 (SM7), 667–692.

Hudson, M., Idriss, I., Beikae, M., 1994. User's Manual for QUAD4M: A Computer Program to Evaluate the Seismic Response of Soil Structures Using Finite Element Procedures and Incorporating a Compliant Base. University of California, Davis, U.S.A.

Idriss, I., Lysmer, J., Hwang, R., Seed, H., 1973. QUAD4: a computer program for evaluating the seismic response of soil structures by variable damping finite element procedures, EERC Report 73-16. University of California, Berkeley, U.S.A.

Ishihara, K., 1996. Soil Behaviour in Earthquake Geotechnics. Oxford Science Publications.

Iwasaki T., Tatsuoka F., Tokida K. and Yasuda S. 1978. A practical Method for Assessing Soil Liquefaction Potential Based on Case Studies at Various Sites in Japan. In: Proceedings of the 2nd International Conference on Microzonation for Safer Construction Research and Application. Vol. 2, pp. 885–896.

Kazama, M., Kataoka, S., Uzuoka, R., 2012. Volcanic mountain area disaster caused by the Iwate-Miyagi Nairiku Earthquake of 2008, Japan. Soils Found. 52 (1), 168–184.

Kawamura, S., Miura, S., 2013. Rainfall-induced failures of volcanic slopes subjected to freezing and thrawing. Soils Found. 53 (3), 443–461.

Khouri N., 1984. Dynamic Properties of Soils (M.S. dissertation). Department of Civil Engineering, Syracuse University.

Kokusho, T., 1980. Cyclic triaxial test of dynamic soil properties for wide strain range. Soils Found. 20 (2), 45–60.

Kokusho, T., 2004. Nonlinear site response and strain-dependent soil properties. Curr. Sci., Spec. Sect.: Geotech. Earthquake Hazards 87 (10), 1363–1369.

Lobo-Guerrero, S., Vallejo, L.E., 2005. Analysis of crushing of granular material under isotropic and biaxial stress conditions. Soils Found. 45 (4), 79–89.

Lobo-Guerrero, S., Vallejo, L.E., 2006. Modeling granular crushing in ring shear tests: experimental and numerical analyses. Soils Found. 46 (2), 147–158.

Menq F.-Y., 2003. Dynamic Properties of Sandy and Gravelly Soils (Ph.D. dissertation). University of Texas, Austin, USA.

Meyer, V.M., Larkin, T.J., Pender, M.J., 2005. Shear strength and dynamic shear stiffness of New Zealand volcanic ash soils. Soils Found. 45 (3), 9–20.

Okur, D., Ansal, A., 2007. Stiffness degradation of natural fine grained soils during cyclic loading. Soil Dyn. Earthquake Eng. 27, 843–854.

Orense, R.P., Zapanta, A., Hata, A., Towhata, I., 2006. Geotechnical characteristics of volcanic soils taken from recent eruptions. J. Geotech. Geol. Eng. 24, 129–161.

Pender, M.J., Wesley, L.D., Larkin, T.J., Pranjoto, S., 2006. Geotechnical properties of a pumice sand. Soils Found. 46 (1), 69–81.

Rollins, K., Evans, M., Diehl, N., Daily, W., 1998. Shear modulus and damping relationships for gravels. J. Geotech. Environ. Eng. 124 (5), 396–405.

Rouse, W., Reading, A., Walsh, R., 1986. Volcanic soil properties in Dominica, West Indies. Eng. Geol. 23, 1–28.

Santamarina, C., Cascante, G., 1996. Stress anisotropy and wave propagation: a micromechanical view. Can. Geotech. J. 33, 770–782.

Santamarina, C., Cascante, G., 1998. Effect of surface roughness on wave propagation parameters. Geotechnique 48 (1), 129–136.

Saxena, S., Reddy, K., 1989. Dynamic moduli and damping ratios for Monterey No.0 sand by resonant column tests. Soils Found., Jpn. Soc. Soil Mech. Found. Eng. 29 (2), 37–51.

Sazzad, Md.M., Suzuki, K., 2011. Effect of interparticle friction on the cyclic behavior of granular materials using 2D DEM. J. Geotech. Geoenviron. Eng. 137 (5), 545–549.

Seed, H., Idriss, I., 1970. Soil Moduli and Damping Factors for Dynamic Analysis, Report, Report No. EERC 70-10. University of California, Berkley, USA.

Seed, H., Wong, R., Idriss, I., Tokimatsu, K., 1986. Moduli and damping factors for dynamic analysis of cohesionless soils. J. Geotech. Eng., ASCE 112 (11), 1016–1103.

Senetakis K., (2011). Dynamic Properties of Granular Soils and Mixtures of Typical Sands and Gravels with Recycled Synthetic Materials (Ph.D. dissertation). Department of Civil Engineering, Aristotle University of Thessaloniki, Greece (in Greek).

Senetakis, K., Anastasiadis, A., Pitilakis, K., 2012a. The small-strain shear modulus and damping ratio of quartz and volcanic sands. Geotech. Testing J. 35 (6), 1–17. http://dx.doi.org/10.1520/GTJ20120073.

Senetakis, K., Anastasiadis, A., Pitilakis, K., 2012b. Dynamic properties of dry sand/rubber (RSM) and gravel/rubber (GRM) mixtures in a wide range of shearing strain amplitudes. Soil Dyn. Earthquake Eng. 33, 38–53.

Senetakis, K., Anastasiadis, A., Pitilakis, K., Souli, A., 2012c. Dynamic behavior of sand/rubber mixtures, Part II: effect of rubber content on G/Go-γ-DT curves and volumetric threshold strain. J. ASTM Int. 9 (2).

Senetakis, K., Anastasiadis, A., Pitilakis, K., Coop, M.R., 2013a. The dynamics of a pumice granular soil in dry state under isotropic resonant column testing. Soil Dyn. Earthquake Eng. 45, 70–79.

Senetakis, K., Coop, M.R., Todisco, M.C., 2013b. Tangential load-deflection behavior at the contacts of soil particles. Geotech. Lett. 3 Issue April-June, pp. 59-66.

Senetakis, K., Coop, M., Todisco, M.C., 2013c. The inter-particle coefficient of friction at the contacts of Leighton Buzzard sand quartz minerals. Soils Found., 53, pp. 746-755.

Sezer, A., Altun, S., Goktepe, A.B., 2011. Relationhips between shape characteristics and shear strength of sands. Soils Found. 51 (5), 857–871.

Sherif, M., Ishibashi, I., 1976. Dynamic shear moduli for dry sands. J. Geotech. Eng., ASCE 102 (11), 1171–1184.

Shibata, T., Soelarno, D., 1975. Stress strain characteristics of sands under cyclic loading. Proc. Jpn. Soc. Civil Eng. 239, 57–65.

Schnabel, P., Lysmer, J., Seed, H., 1972. SHAKE: A Computer Program for Earthquake Response Analysis of Horizontally Layered Sites. Berkeley, University of California, USA.

Stokoe K., Hwang S., Lee N. and Andrus R., 1994. Effects of various parameters on the stiffness and damping of soils at small to medium strains. In: Proceedings of the International Symposium on Pre-failure Deformation Characteristics of Geomaterials, Sapporo, Japan. Vol. 2, pp. 785–816.

Stokoe K., Darendeli M., Gilbert R., Menq F.-Y. and Choi W.-K., 2004. Development of a new family of normalized modulus reduction and material damping curves. In: Proceedings of the NSF/PEER International Workshop on Uncertainties in Nonlinear Soil Properties and their Impact on Modeling Dynamic Soil Response, University of California at Berkeley, Berkeley, California, USA.

Sun, J., Golesorkhi, R., Seed, H., 1988. Dynamic Moduli and Damping Ratios for Cohesive Soils, Report, UCB/EERC-88/15. University of California, Berkeley, USA.

Tanaka, Y., Kudo, K., Yoshida, Y., Ikemi, M., 1987. A Study on the Mechanical Properties of Sandy Gravel-Dynamic Properties of Reconstituted Sample, Report, Report U87019. Central Research Institute of Electric Power Industry (in Japanese).

Tatsuoka, F., Iwasaki, T., 1978. Hysteresis damping of sands under cyclic loading and its relation to shear modulus. Soils Found., Jpn. Soc. Soil Mech. Found. Eng. 18, 25–40.

Thornton, C., 2000. Numerical simulations of deviatoric shear deformation of granular media. Geotechnique 50 (1), 43–53.

Vilhar, G., Jovicic, V., Coop, M.R., 2013. The role of particle breakage in the mechanics of a non-plastic silty sand. Soils Found. 53 (1), 91–104.

Vucetic, M., Dobry, R., 1991. Effect of soil plasticity on cyclic response. J. Geotech. Eng. 117 (1), 89–107.

Wesley L., 2003. Geotechnical properties of two volcanic soils. In: Proceedings of the New Zealand Geotechnical Society sysmposium, Tauranga.

Wang, J., Yan, H., 2011. On the role of particle breakage in the shear failure behavior of granular soils by DEM. Int. J. Numer. Anal. Methods Geomech., 37 (8), pp. 832-854.

Wang, J., Yan, H., 2012. DEM analysis of energy dissipation in crushable soils. Soils Found. 52 (4), 644–657.

Wichtmann T., Hernandez M., Martinez R., Graeff D., Triantafyllidis Th., 2011. Estimation of the small-strain stiffness of granular soils taking into account the grain size distribution curve. In: Proceedings of the 5th International Conference on Earthquake Geotechnical Engineering, Santiago, Chile.

Xenaki, V., Athanasopoulos, G., 2008. Dynamic properties and liquefaction resistance of two soil materials in an earthfill dam – laboratory test results. Soil Dyn. Earthquake Eng. 28 (8), 605–620.

Yao, Y.P., Yamamoto, H., Wang, N.D., 2008. Constitutive model considering sand crushing. Soils Found. 48 (4), 603–608.

Yimsiri, S., Soga, K., 2000. Micromechanics-based stress–strain behaviour of soils at small strains. Geotechnique 50, 559–571.

Zhang, J., Andrus, R., Juang, C., 2005. Normalized shear modulus and material damping ratio relationships. J. Geotech. Geoenviron. Eng., ASCE, 131; 453–464.